Selective synthesis of γ-valerolactone from levulinic and formic acid over ZnAl mixed oxide

*Meriem N.E. H. Belguendouz[1,2], Juan Gancedo[1], Paula Rapado[1], David Ursueguía[1], Yolanda Patiño[1], Laura Faba[1], Abdellah Bahmani[2], Eva Díaz[1], Salvador Ordóñez[1]**

[1]Catalysis, Reactors and Control Research Group (CRC), Dept. of Chemical and Environmental Engineering, University of Oviedo, Oviedo 33006, Spain

[2]Laboratory of Chemistry of Inorganic Materials and Applications (LCMIA), University of Science and Technology of Oran - Mohamed Boudiaf - USTO-MB, BP. 1505 Oran, El- Mnouer-31035, Algeria

*e-mail: sordonez@uniovi.es, Tel: +34 985 103 437; Fax: + 34 985 103 434

Abstract

After testing different mixed oxides, a very promising catalyst to obtain γ-valerolactone from levulinic acid and formic acid is proposed in this work: a ZnAl hydrotalcite-derived material. Optimum conditions (T=140ºC, FA/LA=5/1, aqueous phase stirred batch reactor) excel results previously proposed in the literature, combining high activity (>87 %) and selectivity (90 % GVL yield) with remarkable stability, the reaction being performed at mild conditions and using a highly available and cheap catalyst.

A detailed mechanistic with its kinetic study was accomplished for this optimum catalyst, considering that formic acid decomposition is the limiting step following a second-order kinetic, and the FA dehydration to AL is a pseudo-first-order reversible step. Angelica-lactone is identified as the main by-product and the precursor for the formation of light organic deposits, the main responsible for the slight deactivation observed during the experiments in absence of reactivation procedure.

Keywords:

Dehydrogenation, angelica lactone, renewable hydrogen, bioplatform molecules

1. Introduction

The γ-valerolactone (GVL) is considered as one of the top value-added chemicals obtained from biomass [1,2]. Its high versatile character attracts attention, with potential uses as a green solvent [3,4]. Due to its sweet and herbaceous odour, it is also relevant for the food and cosmetic industries [5,6] and it is also an interesting intermediate to obtain adhesives, olefins, polymers, and other products [7-9]. In most cases, traditional routes to produce these products require petroleum derivatives, being the substitution by the GVL an excellent opportunity to advance in the Principles of Circular Economy. The GVL also has promising applications in the liquid fuel field, since long-chain alkanes (C8-C18) can be produced from it, blending gasoline, diesel, and aviation fuels with concentrations up to 10 %, without modifying the octane index or requiring the adaptation of combustion engines [10,11].

The catalytic hydrogenation of levulinic acid (LA) is the main route proposed to obtain GVL from a renewable source. LA is produced by the decomposition of 5-HMF under acidic conditions, being its availability guaranteed since it derives from hexoses, the main monomer of lignocellulosic biomass [12]. Regardless of the hydrogen source used for the LA upgrading to GVL (molecular H_2 or other molecules undergoing decomposition reactions yielding H_2), two different pathways are proposed in the literature, involving 4-hydroxyvaleric acid (HVA) or angelica lactone (AL) intermediates, as a function of the first stage taking place: HVA hydrogenation or AL dehydration [13,14]. According to the literature, the first route is more relevant at low temperatures (mainly lower than 150ºC), whereas the second one is the predominant at higher temperatures (>150ºC) or in presence of strong acid sites [15,16]. In both

cases, hydrogenation is identified as the rate-determining step [17]. There is a wide bibliography about this procedure using molecular hydrogen, including noble metals and transition ones [15,18-21]. However, the direct use of hydrogen for these steps is not fully attractive because of its high cost and the safety constraints derived from its flammable character.

Different hydrogen donors, such as formic acid (FA) [22-24] and small alcohols (mainly ethanol and 2-propanol) [25,26] are proposed as alternatives to molecular H_2. Formic acid is the most promising one since it is co-produced together with the levulinic acid (equimolar production of both acids in the acid hydrolysis of cellulosic biomass by rehydration of 5-hydroxymethylfurfural [12,27]) and because it can be effectively decomposed into CO_2 and H_2 without producing any side-compound in the liquid phase [24]. This step is critical to the overall process because it determines the efficiency of the hydrogen supply [28]. This catalytic decomposition must be very selective, preventing the hydration decomposition that could produce water and carbon monoxide as products [29]. In addition to the subsequent decrease in the hydrogenation activity, this CO produced could affect the catalytic stability promoting reversible poisoning of metal nanoparticles [30]. Thus, using FA as a hydrogen source for the levulinic acid hydrogenation requires a more complex catalyst, including different functionalities: transition metals and/or basic sites for the FA dehydrogenation, acid sites for the LA dehydration, and metal sites for the AL hydrogenation.

Many heterogeneous catalysts have been proposed in the literature, highlighting the good results obtained with precious metals supported on acid materials, such as

Au/ZrO_2 (99 % of GVL yields in less than 6 h at 150°C) [31], and Ru/ZrO_2 (100 % of LA conversion, 73 % of GVL yield, after 12 h at 150°C) [32]. The high cost of these catalysts promotes the development of bimetallic ones, including precious and nonprecious metals (mainly Ni and Cu), reaching GVL yields higher than 70 % [33,34]. In all the cases, metal dispersion and particle size are highlighted as the key parameters. Metal leaching due to the acidic medium, particle sintering, poisoning by CO, and coke deposition on the metal particles are reported as typical deactivation causes for this reaction [24], being promoted by the presence of reduced metals. This fact endorses the screening of non-reduced materials, such as metal oxides.

Mixed oxides have been deeply studied in different biomass upgrading reactions [35,36], combining low cost and good activity since an optimum selection of transition metals can introduce different active sites, increasing catalyst versatility. Nevertheless, the use of metal-free materials for this reaction is still anecdote, despite the promising results obtained for Mg-Al mixed oxides working in the gas phase (100 % conversion, 98 % yield of GVL at 270°C) [37]. These results are controlled by a relevant deactivation, caused by the coke deposition on the basic sites, suggesting the use of more acidic materials as a good alternative.

This works aims to evaluate the catalytic activity of different hydrotalcite-like compounds, studying different oxides combination (Co, Ni, Fe, Al, Zn) with the objective of maximizing both, the activity and stability on the levulinic liquid-phase acid hydrogenation to obtain GVL using formic acid as a renewable hydrogen source. These metals were individually chosen according to their well-known activity the single steps involved in this reaction: dehydrations (Fe, Al) [38,39] and

hydrogenation/dehydrogenation reactions, in the cases of Co and Ni [40,41]. Moreover, working in liquid phase is more attractive than in the gaseous one from the point of view of the sustainability of the process. In this context, the selective decomposition of formic acid in absence of any reduced metal is assumed as the most difficult step to promote. The high activity of Zn^{2+} in the selective decomposition of formic acid via dehydrogenation has been previously reported [29], so Zn is also considered as a good candidate for the optimum catalyst. Different metal oxide pairs were selected trying to identify the best combination of these functionalities in the global process since there is not a good agreement in the literature about the prevalence of dehydrogenations or hydrogenation steps [24].

2. Experimental

2.1. Catalyst preparation

The hydrotalcite-like compounds were synthesized by a co-precipitation method at low super-saturation conditions, using the corresponding nitrates as precursors: $Ni(NO_3)_2{\cdot}6H_2O$, $Al(NO_3)_3{\cdot}9H_2O$, $Co(NO_3)_2{\cdot}6H_20$, $Fe(NO_3)_3{\cdot}9H_2O$ and $Zn(NO_3)_3{\cdot}9H_2O$. The XY hydroxides precipitation ($Ni(OH)_2/Fe(OH)_3$, $Zn(OH)_3/Al(OH)_3$, $Co(OH)_2/Al(OH)_3$ and $Ni(OH)_3/Al(OH)_3$), all of them with an X/Y theoretical molar ratio of 2/1, was assisted by Na_2CO_3, using NaOH to regulate the pH during all the process. All the salts and the NaOH were purchased by Prolabo. In a typical batch, 100 mL of the X and Y nitrates solution (2 M and 1 M, respectively) were dropwise added to 100 mL of distilled water containing 2 M Na_2CO_3. This process was done under fast stirring at a constant pH of 10, the pH being regulated by the continuous addition of the 1 M NaOH solution. Once

the gel is obtained, it is aged for 24 h at 80°C before centrifugation, the solids being washed with distilled water until neutral pH. The hydrotalcites-like materials were dried in an oven for 24 h (70°C) before the air-treatment (100 $mL \cdot min^{-1}$), with a temperature slope of $5°C \cdot min^{-1}$ up to 500°C. The final temperature is held for 6 hours. In the manuscript, the catalysts were identified with their corresponding metals to an easy identification: NiFe, ZnAl, CoAl, NiAl.

2.2. Catalysts characterization

The bulk chemical composition of the fresh catalysts was determined using an Agilent 7700x inductively coupled plasma mass spectrometer (ICP-MS), once the samples were dissolved in 1 % HNO_3 (1:250), using Rh as the internal standard. This procedure was also applied to check a possible metal leaching during the process, analysing the fraction of metals dissolved in the reaction medium once the solids were removed by filtration, as well as the composition of the solid catalyst after different cycles.

The textural properties were determined by N_2 physisorption at 77 K, using an ASAP 2020. BET and BJH models were used to determine the surface area and pore volume, respectively. The crystallographic structures of the hydrotalcite-like materials were determined by X-ray diffractometry (XRD) in a Philips PW 1710 diffractometer, working with the Cu-Kα line (λ=0.154 nm) in the 2θ range of 5-85°, using a scanning rate of $2° \cdot min^{-1}$. A similar procedure was carried out with spent samples, to identify any possible modification in their crystalline structures during the reaction.

The amount and strength distribution of basic and acidic sites were determined by temperature-programmed desorption (TPD) of CO_2 and NH_3, respectively, in a Micromeritics TPD/TPR 2900 coupled to a Pfeiffer Vacuum Omnistar quadrupole mass spectrometer. Samples (20 mg) were heated to 383 K with helium flow (20 mL·min^{-1}) for 1 h to remove any compound physisorbed on the surface. Then, the catalytic surface was saturated at room temperature with the probe molecule (2.5 % in He, 20 mL·min^{-1}, 20 min). Once the oversaturation is removed (stabilization period of 2 h in 20 mL·min^{-1} He flow), the probe molecule desorption is monitored from room temperature to 873 K, with a temperature slope of 5 K·min^{-1}. The distributions of acidic and basic sites were calculated by deconvolution of the desorption curves using the procedure outlined in previous works [42,43].

The same instrument was used to determine the reduction temperature of these catalysts (TPR), to check if the oxidation state of these metals could be altered because of the reaction conditions. Once the surface is cleaned (same procedure as explained for the TPD), the analysis was carried out feeding 20 mL·min^{-1} of 10 % H_2 in He, monitoring the H_2 signal from room temperature to 823 K, with a slope of 5 K·min^{-1}.

Solid deposits on the surface of spent catalysts were identified by oxidation at programmed temperature (TPO) analyses, carried out in the same equipment as the TPD and TPR. The CO_2 signal (m/z=44) is followed by mass spectrometry whereas 20 mg samples are submitted to an increasing temperature (5ºC·min^{-1}) up to 873 K.

2.3. Reaction studies

Experimental reactions were carried out in a 0.5 L batch reactor (Autoclave Engineers EZE Seal), equipped with a stirrer, a PID temperature controller, and a backpressure regulator. In a typical experiment, 250 mL of an aqueous solution of levulinic acid was fed (98 %, Sigma Aldrich), with a reactant concentration of 19.3 $g \cdot L^{-1}$ (0.166 $mol \cdot L^{-1}$). Once the solution is pre-heated to 343 K, a variable concentration of formic acid (>98%, Sigma Aldrich), from 6.3 to 31.5 $mL \cdot L^{-1}$ (from 0.166 to 0.664 $mol \cdot L^{-1}$), is also introduced, obtaining initial LA/FA molar ratios of 1/1, 2/1, 3/1, 4/1 and 5/1. Simultaneously, 1 g of catalyst is added, the reactor being closed and purged with N_2 three times. The reaction temperature is fixed at the set point in the PID, establishing 15 bar of inert pressure (N_2) and 1000 rpm of stirring. This stirring speed was chosen after preliminary tests to check its influence on the mass transfer, concluding that constant results are obtained once the stirring speed is higher than 800 rpm. Different temperatures were studied, from 353 to 473 K. The inert pressure prevents possible evaporation at the reaction conditions, also allowing the periodical sampling.

Liquid samples were withdrawn by the sample port to study the temporal evolution of reactant and product concentrations during the reaction time. Once filtered, samples were analysed by gas chromatography using a mass spectrometer detector (GC-MS), in a Shimadzu QP2010 with a 30 m long TRB-5MS capillary column. The signal calibration was carried out using commercial samples of levulinic acid (LA), GVL, angelica lactone (AL), and formic acid (FA). Gaseous samples were taken using a gas bag, the gases being analysed by a mass spectrometer (Pfeiffer Vacuum Omnistar). This procedure was only used to corroborate the presence of molecular hydrogen from the formic acid

decomposition, being not reliable for quantitative analysis. Thus, the temporal evolution of hydrogen is calculated as a mass balance considering the theoretical decomposition of formic acid and the hydrogen consumed to obtain the GVL.

Experiments with the different catalysts were repeated twice, the data shown in the results and discussion section 3.1 being the average value of both tests, with a standard deviation lower than 6 % in all the cases. Results were analysed according to the levulinic acid and formic acid conversions, the product yields, and the carbon balance closure according to the following equations (1-3):

$$Conv = \frac{C_{i,t} - C_{i,0}}{C_{i,0}} \cdot 100\ (=)\ \% \qquad [1]$$

$$Yield, \Psi = \frac{C_{j,t}}{C_{LA,0}} \cdot 100 (=)\ \% \qquad [2]$$

$$CB = \frac{5 \cdot C_{LA,t} + C_{FA,t} + 5 \cdot C_{AL,t} + 5 \cdot C_{GVL,t}}{5 \cdot C_{LA,0} + C_{FA,0}} \cdot 100 (=)\ \% \qquad [3]$$

Where “i” corresponds to the reactants, formic (FA) or levulinic acid (LA), as a function of the compound to be evaluated. In the yield equation, “j” indicates the possible products, angelica lactone (AL) or γ-valerolactone (GVL). This parameter is measured as a function of the initial levulinic acid since the evolution of this compound is directly related to the main reaction, whereas the formic acid can be independently decomposed.

2.4. Kinetic studies

Reactions conditions were chosen to guarantee an intrinsic kinetic control, with a small and narrow particle size distribution (50-80 μm), and a high stirring speed (1000 rpm). Moreover, the presence of internal mass-transfer effects has been discarded by a theoretical consideration consisted of a kinetic model derivation considering the liquid-solid mass transfer and the Thiele modulus-based efficiency factor for internal diffusion [44]. Even at the most restrictive conditions (ZnAl, 200ºC), the value obtained is more than one order of magnitude lower than the minimum value required to consider these mass transfer phenomena as limiting step (0.0112 *vs.* 0.1 as limit). The diluted system, high stirring, and low reaction enthalpy of this reaction (calculated as 350 $kJ \cdot mol^{-1}$, using HYSYS software) discard any heat transfer limitation.

Based on these studies, the reactions can be analysed in terms of intrinsic chemical kinetic. MATLAB code was used to perform all the calculations and to solve the set of ordinary differential equations ("ode45"). The fitting of the unknown parameters was accomplished by the least-square method using the "lsqcurvefit" function and the Levenberg-Marquardt algorithm.

3. Results and Discussion

3.1. Catalytic screening.

The initial screening of the catalytic activity was carried out using a FA/LA molar ratio of 4/1 and 200^{o}C. These conditions were chosen to guarantee a severity enough to produce the formic acid decomposition, considering that temperatures higher than

140^{o}C are required to observe this decomposition to a high extend, even when noble metals were used as catalysts [24]. A previous blank experiment discards the presence of non-catalytic reaction (levulinic acid conversion lower than 4 % after 6 h in absence of catalyst). In the same way, the requirement of formic acid as a hydrogen donor was also proved since negligible conversion is observed after 6 h when the reactions are carried out without feeding the formic acid. On the other hand, the absence of metal reduction was corroborated by individual programmed-temperature reduction analyses (TPR) of these materials, requiring 336, 372, 500^{o}C to observe the reduction of CoAl, NiFe, and NiAl, without observing any reduction in the ZnAl in the temperature range analysed (30 – 550^{o}C). These results, shown in Figure S1, discard any role of metal nanoparticles since the reaction temperature (200^{o}C) is lower than these values. Thus, catalyst performance will depend only on the mixed oxides activity.

Experimental results after 6 h reaction time are compared in **Figure 1**. Reaction results will be discussed in terms of the catalytic properties reported in **Table 1**, where the experimental molar ratio between metals (ICP results), the morphological analyses, and the acidity and basicity are included. The corresponding TPD graphs are included in the supplementary information (Fig.S2). To complete the analysis of these results, the evolution of the catalytic structure measured by XRD is shown in **Figure S3**.

CoAl mixed oxide provides a high levulinic acid conversion (75 %), with a good match between this value and the GVL production (74 %). This result, as well as the good carbon balance closure, discards any side reaction catalysed by this material. Thus, this material was not further considered because of the high relevance of homogeneous routes. The low formic acid conversion reached with NiAl (0.018 mol·L^{-1}, 3%)

considering the amount of GVL detected (0.069 mol·L^{-1}) suggests that this catalyst allows obtaining H_2 from another source, but its activity for the formic acid decomposition is very low (expected formic acid conversion of 11.1%).

With this material, despite the significant LA conversion (69 %), the GVL selectivity is lower than the corresponding to the other catalysts (<45 %). This result, as well as the low carbon balance (75 % after 6 h), suggests that NiAl catalyses non-desired reactions, or that it promotes the permanent adsorption of compounds involved in the reaction. An intermediate behaviour is observed when using NiFe, with a good correspondence between levulinic and formic acid conversions (68.4 and 17.7 %). The good carbon balance closure discards relevant side reactions or strong adsorptions, but the results are conditioned by the catalytic lixiviation (homogeneous mechanism).

Table 1: Physicochemical properties of mixed oxides

Catalyst	X/Y ratio (ICP)	Metal leaching (ppm)	Surface area (m^2/g)	Pore volume (cm^3/g)	Pore diameter (nm)	Acidity, µmolNH_3/g [Temp., K]	Basicity, µmolCO_2/g [Temp., K]
CoAl	2.16	Co: 798 Al: <2	137	0.39	11	295 [371] 400 [429] 272 [669]	35 [341] 46 [377] 98 [501]
ZnAl	2.06	Zn: 87 Al: <2	24	0.14	23	438 [365] 454 [678]	25 [365] 10 [486]
NiAl	1.96	Ni: 1527 Al: <2	277	0.52	14	396 [378] 1174 [464]	347 [528] 289 [691]
NiFe	1.99	Ni: 922 Fe: 1426	155	0.52	16	297 [356] 432 [400] 923 [495] 232 [689]	285 [330] 709 [354] 1338 [403]

The best results are obtained using ZnAl as catalyst. This material shows the maximum LA conversion (97 %), with a good correspondence with the GVL yield (84 %) and a

good carbon balance closure (>92 %), obtaining angelica lactone yields lower than 4 %. All these results can be justified considering the characterization properties of this material, as explained below.

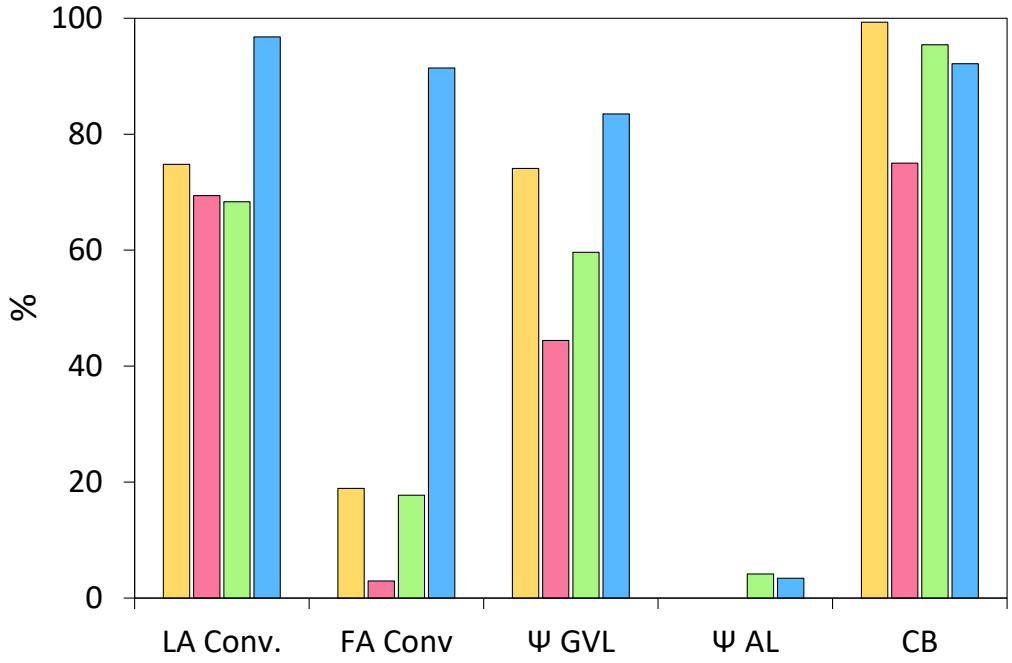

Figure 1: Main results (conversions and yields) obtained after 6 h of reaction between levulinic acid and formic acid, at 200ºC as function of the catalyst used. Data corresponds to: (■) CoAl, (■) NiAl, (■) NiFe and (■) ZnAl mixed oxides.

The absence of any side reaction when working with CoAl could be anticipated, considering the low basicity of this material since strong basic sites are identified as the main precursors of side reactions in this reaction [45]. The absence of any intermediate detected in relevant amount (only small quantities of angelica lactone during the first 2 h of reaction) also indicates a high hydrogenation activity of this material. The hydrogenation activity of cobalt oxides has been previously observed in the literature [43]. The acidity of this material (almost 1 $mmol \cdot g^{-1}$) is congruent with its dehydration capacity, but this step is considered as the limiting one in this case since

total hydrogenation of the angelica lactone is observed. Despite these good results, this material must be rejected because of its high leaching (almost 800 ppm of Co^{2+} detected in the liquor mixture). XRD analyses revealed that the mixed oxide structure (marked by a low crystallinity, with only some small and wide peaks) is stable during the reaction, without detecting a relevant evolution of any crystalline phase. Thus, the rehydration to obtain the HT-like precursor is discarded in this case. The high Co leaching is not detected by XRD since the peaks detected in the fresh and spent catalysts correspond to alumina phases. In water, the pair Co^{2+}/Co^{3+} has a significant redox activity [46], in such a way that its action as a heterogeneous catalyst could be reinforced by homogeneous processes, improving the formic acid dehydrogenation [40].

To demonstrate this fact, a separate experiment was carried out using as a solvent the reaction medium recovered after 6 h of reaction, once filtered to remove any CoAl solid particle. The reaction was done feeding the same amount of formic and levulinic acids but without introducing any solid catalyst. Final conversion after 6 h was 35 %, with 22 % of GVL produced, corroborating the significant homogeneous catalytic activity of dissolved Co^{2+}, suggesting the previously mentioned redox activity as the responsible of this conversion, following a mechanism conditioned by the intermediate formation of cobalt complexes. Due to this finding, this catalyst is not further considered in this work since, according to the Principles of the Green Chemistry, this work is focused on heterogeneous catalysis and not the homogeneous one.

As to the NiAl, the low formic acid decomposition indicates preferential adsorption of levulinic acid over the FA on the catalytic surface, which prevents the interaction

required to promote the FA dehydrogenation. Water is the only alternative H_2-donor in the reaction system. The Ni oxidation with the simultaneous water decomposition has been previously proposed in the literature, obtaining moderate amounts of H_2 [47]. This decomposition is a redox process congruent with the oxidation of Ni species (from NiO to Ni_2O_3) observed by XRD when the fresh and spent NiAl materials are compared. The TPO analysis of the spent catalyst, included in the supplementary information, Fig.S4, discards the promotion of permanent adsorption of compounds involved in the reaction since the oxidation temperatures of the main peaks (420 and 495^{o}C) are significantly higher than the corresponding to the angelica lactone or GVL adsorbed on the catalytic surface (210 - 250 ^{o}C), whereas the adsorption of levulinic acid was not significant enough to produce any signal. These adsorption tests were done keeping the fresh catalysts suspended on a solution of the maximum amount of each compound that could be obtained at these reaction conditions, to guarantee the most favourable conditions to observe any possible adsorption.

Concerning the side reactions, the deactivation involving angelica lactone (or angelica lactone degradation products) adsorption is proposed as the main one. This hypothesis, also proposed by other authors [45,48], is congruent with the chemical properties of this compound, especially the presence of unsaturated C-C bonds. Thus, the high total acidity of this mixed oxide (1.5 $mmol \cdot g^{-1}$) anticipates a high dehydration activity, producing angelica lactone, whereas the presence of strong basic sites promotes adsorption processes once the hydrogenation is limited by the H_2 production. In addition to this undesired behaviour, the catalytic leaching is also a relevant drawback of this material. The ICP analysis of the reaction medium indicates the presence of Ni dissolved in a relevant amount (>1500 ppm). In the same way, XRD

provided in Fig. S3, suggests the presence of both changes on the Ni oxidation state and in the crystallographic structure during the reaction. The homogeneous activity was tested using the reaction medium for a second cycle after removing the solid phase by filtration, obtaining 35 % of levulinic acid converted after 6 h. Thus, the homogeneous catalysis is even more marked than with CoAl.

The absence of strong basic sites on NiFe despite the significant total amount of these sites is congruent with the low relevance of angelica lactone adsorption and possible oligomerization, obtaining a good carbon balance (95 %). In the same way, the low amount of strong acid sites (less than 13 % of the total ones) justifies the presence of angelica lactone in the final samples, without obtaining the total hydrogenation of this intermediate. ICP results indicate partial leaching of the solid catalyst, observing both Ni and Fe in the reaction medium, without a significant influence in the catalytic crystalline structure, according to the good correspondence between fresh and spent material (XRD, Fig. S3). The homogeneous catalysis is also relevant in this case, with almost 20 % of levulinic acid conversion. Because of these results, this mixed oxide cannot be proposed for further studies.

Finally, the best results were obtained with ZnAl. The total formic acid conversion reached with this material indicates that this material is the only one catalysing this decomposition at a large extent, in such a way that the hydrogen availability is not a limiting step in the process. In other words, there is preferential adsorption of FA on the catalytic surface, promoting its decomposition, and the global activity is then conditioned by the inferior adsorption of LA. This hypothesis was corroborated by analysing the gas phase after 2, 4 and 6 h of reaction, observing an increasing signal of

H_2 once the gas bag is analysed by mass spectrometry, included in the supplementary information (Fig. S5). As explained in the experimental section, this procedure was applied to identify the presence of hydrogen, but this procedure does not allow to perform quantitative analysis. Then, the hydrogen concentration is calculated by a mass balance considering the formic acid decomposition and the H_2 consumed by the angelica lactone hydrogenation. The temporal evolution of hydrogen is shown in Figure 2, being discussed on the reaction mechanism section. The high affinity of formic acid to the ZnO surface and its selective decomposition into H_2 and CO_2 has been previously reported in the literature [29]. The medium-strength acidity of this material partially explains the high dehydration capacity, but differences among materials are not so relevant to justify the differences in LA conversion. An equilibrium dehydration-hydration is then suggested, the high amount of H_2 available with this material being the responsibility for the equilibrium displacement because of AL consumed by hydrogenation, reaching an almost total LA conversion. However, the presence of angelica lactone also indicates that the hydrogenation ability of this mixed oxide is slightly limited. The lack of basicity is congruent with the absence of any side reaction. The stability of this mixed oxide is corroborated by the XRD spectra, obtaining a clear mixed oxide structure with a similar aspect before and after the reaction, in which only some peaks related to ZnO are identified. In good agreement with these results, the metal lixiviation is negligible, also discarding the homogeneous reaction. According to these data, ZnAl mixed oxide is identified as the optimum catalyst for the transformation of LA into GVL using formic acid as the H_2 source.

3.2. Reaction mechanism

In general, two different reaction routes have been proposed in the literature for the levulinic acid transformation into GVL, involving the 4-hydroxyvaleric acid (HVA) or the angelica lactone intermediates, as function of the most active sites present in the catalysts [13,14]. Thus, if the hydrogenation steps are the most favoured (typically when a reduced metal is used), the HVA intermediate is detected, its subsequent dehydration being the second step for obtaining the GVL. On the contrary, when acid-catalysed steps are favoured, the levulinic acid undergoes an initial dehydration, obtaining the angelica lactone (isomerization equilibrium between the alpha and beta isomers). This is the most typical mechanism in absence of any reduced metal particle mainly when using an H-donor different from the molecular H_2, since the hydrogenation requires a previous decomposition of the chemical compound used as hydrogen source [14]. Experimental results are in good agreement with this discussion, without detecting the HVA in any sample. The formic acid decomposition is considered as an independent reaction. This hypothesis was experimentally tested in separate experiments performed with the ZnAl catalyst, feeding only formic acid. A continuous decreasing trend of FA concentration is observed, in good agreement with the previous assumption. The temporal profile of this experiment is shown in **Figure 2a**, reaching more than 90 % of conversion in less than 4 h**.** In previous literature about this decomposition on ZnO [29], the H_2 formation is demonstrated as a bimolecular reaction, reporting thermodynamic data to corroborate the prevalence of this mechanism over the unimolecular one. In a first step, the formic acid is dissociatively adsorbed, yielding a hydrogen atom adsorbed on an oxygen atom, a basic site, of the ZnO, and a formate anion adsorbed by a bridge bond with two consecutive metal sites,

obtaining a formate complex. A second formic acid acts as hydrogen-bonding cocatalyst for HCOO* decomposition, producing CO_2 and H_2 and obtaining a second formate complex [49]. This bimolecular mechanism has been experimentally corroborated analysing the adjustment of temporal decomposition of formic acid in terms of ln [FA] and 1/[FA] vs. time. These plots are included in the supplementary information (**Fig. S6**), observing a better fit when considering the second-order kinetic than with the first-order one.

The presence of Al in two materials tested with so different behaviour observed (CoAl and ZnAl) indicates that the formic acid adsorption selectively occurs on Zn^{2+} sites. Independently, LA is adsorbed on an acid site of the ZnAl mixed oxide, specifically binding its hydroxyl oxygen of the carboxylic group on the coordinatively unsaturated metal site, producing the dehydration with the subsequent cyclization, reaching the AL [50]. The results obtained in this paper do not allow determining the prevalence of any metal site, presuming that the LA adsorption could occur both, on Al and Zn sites, maybe with the predominance of Al sites because of their slightly higher acidity of θ-Al_2O_3 in comparison to the ZnO, (0.30 vs. 0.25 $mmol \cdot g^{-1}$) according to the literature [51,52]. The competitive character of both adsorptions (formic and levulinic acid) on Zn sites explains the slightly faster trend observed in the evolution when only FA is fed in comparison to reaction conditions.

The LA adsorption is considered as weak, the acid dehydration to produce the AL is a reversible reaction. This assumption is in good agreement with literature findings [50], and it was also experimentally corroborated. Thus, angelica lactone was fed as reactant (together with the formic acid, keeping constant the ratio 4/1) in a specific

reaction using ZnAl as the catalyst, showing the temporal profile in **Figure 2b**. After 4 h of reaction at 200^{o}C, 92.6 % of conversion is obtained, detecting both GVL and LA as products (50.9 an 8.70 % selectivity, respectively). The carbon balance closure decreases to 67 %, suggesting the presence of side reactions involving AL. The GVL profile follows a continuously rising trend, in good agreement with the anticipated profile of a final product. However, the LA reaches a maximum of 13.5 % after 2 h, decreasing at longer times to a stable 5 % after 5 h, when the AL conversion is stabilized around 95 %. These results are congruent with an equilibrium between these two species. In the same way, an experiment with GVL as reactant discards any side reaction or reversible decomposition into AL, HVL or LA, since no GVL disappearance is observed after 6 h. Therefore, hydrogenation is considered as an irreversible step.

Once both reactants are adsorbed on neighbour sites, the reaction occurs, producing the GVL. If these sites are not close enough the stable adsorption of AL could produce oligomerization side reactions.

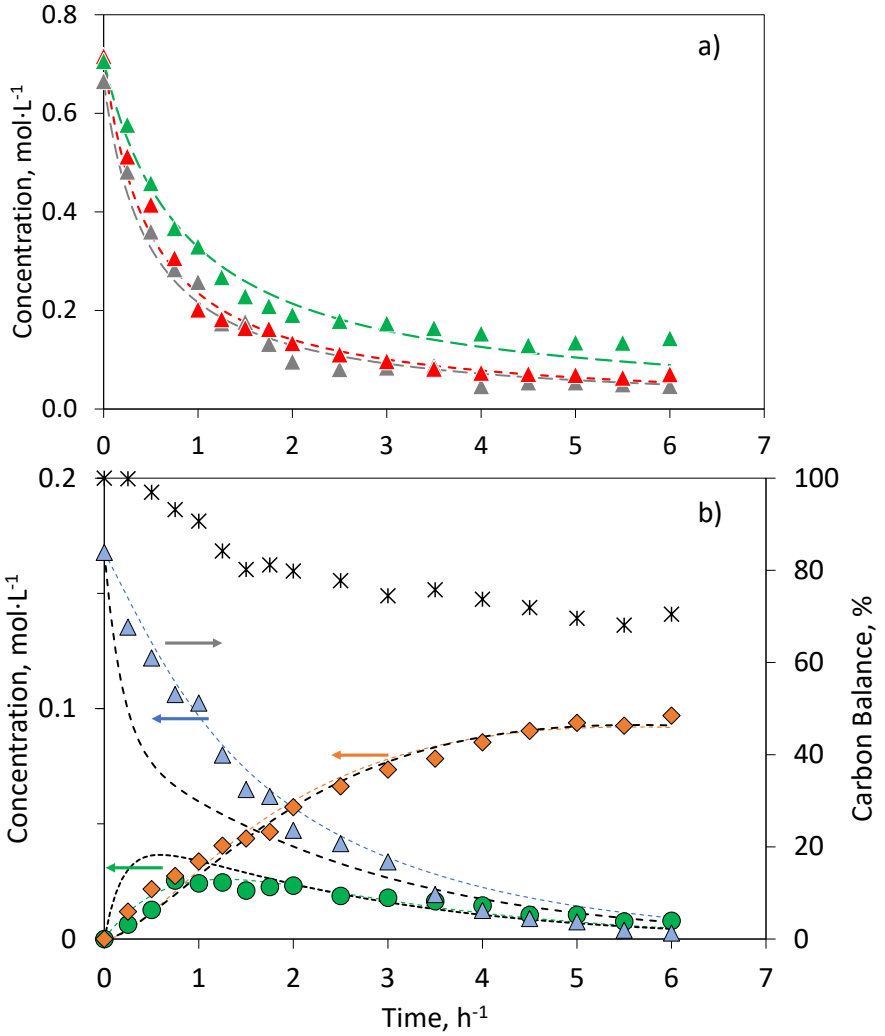

Figure 2: a) Comparative evolution of formic acid (FA) decomposition at 200°C catalysed by ZnAl when feeding only FA (grey), FA and levulinic acid (red), and FA and angelica lactone (green); b) Temporal profiles obtained in the angelica lactone (AL) hydrogenation at 200 °C using ZnAl as catalyst. Symbols: (▲) angelica lactone; (●) levulinic acid; (◆) GVL; and (✳) carbon balance. In both cases, symbols correspond to experimental points, broken lines with fitted values. Black lines correspond to simulations done with LA+FA kinetic parameters, and coloured lines to the data fitting of this experiment.

According to the proposed mechanism, summarized in **Scheme 1**, the temporal evolution of all the compounds involved in the reaction (formic acid, FA; levulinic acid,

LA; angelica lactone, AL; and γ-valerolactone, GVL) could be mathematically expressed as follows:

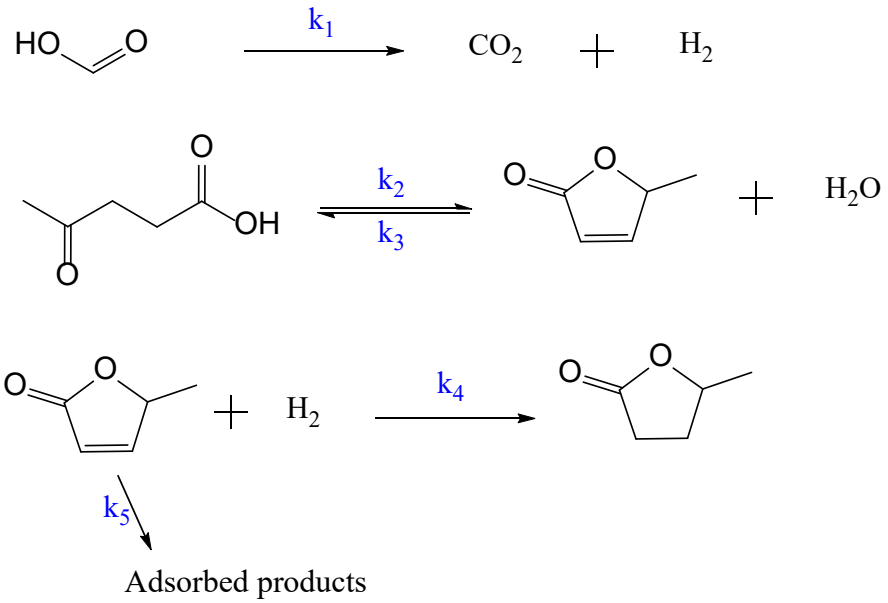

Scheme 1: General kinetic mechanism proposed for the catalytic transformation of levulinic acid into γ-valerolactone using formic acid as H_2 source.

$$\frac{d[FA]}{dt} = -k_1 \cdot [FA]^2 \qquad [4]$$

$$\frac{d[LA]}{dt} = -k_2 \cdot [LA] + k_3 \cdot [AL] \qquad [5]$$

$$\frac{d[H_2]}{dt} = k_1 \cdot [FA]^2 - k_4 \cdot [AL] \cdot [H_2] \qquad [6]$$

$$\frac{d[AL]}{dt} = k_2 \cdot [LA] - k_3 \cdot [AL] \; - k_4 \cdot [AL] \cdot [H_2] - \; k_5 \cdot [AL] \qquad [7]$$

$$\frac{d[GVL]}{dt} = k_4 \cdot [AL] \cdot [H_2] \qquad [8]$$

The first-order proposed for the side reactions contrasts with the oligomerization nature. Higher orders were tested obtained significantly worse adjustments, discarding then the direct oligomerization as the deactivation route. This deactivation is then

explained by the strong adsorption of angelica lactone and other unsaturated compounds, such as pentenoic acid, that could be produced by the AL dissociation. The strong adsorption of this carboxylate ion has been previously proposed in the literature [48]. The unsaturated character of these compounds could help the oligomerization once adsorbed, obtaining carbonaceous deposits that promote the deactivation. Based on this, hereinafter this side reaction is indicated as oligomerization. The kinetic rates obtained are $k_1 = 7.9 \cdot 10^{-4}$ L·mol^{-1}·s^{-1}; $k_2 = 7.3 \cdot 10^{-4}$ s^{-1}; $k_3 = 7.4 \cdot 10^{-4}$ s^{-1}; $k_4 = 4 \cdot 10^{-2}$ L·mol^{-1}·s^{-1}; $k_5 = 4 \cdot 10^{-4}$ s^{-1}, with a global correlation index of 0.992. The good correspondence between experimental and fitted values is displayed in **Figure 3**.

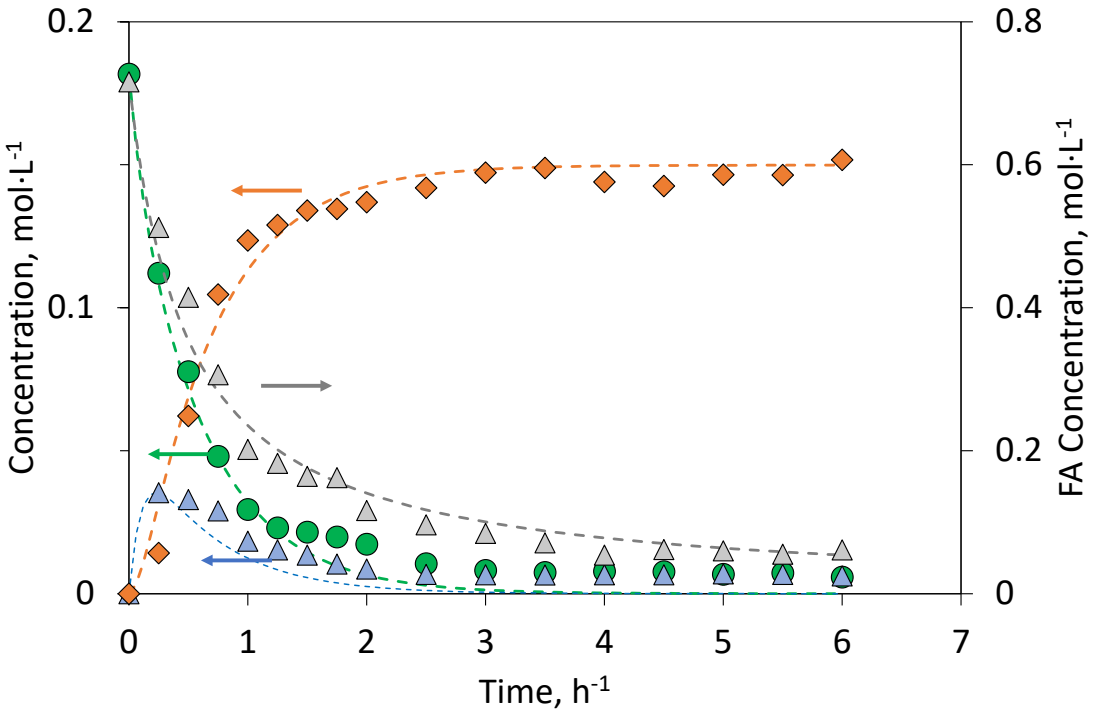

Figure 3. Temporal evolution of compounds involved in the LA transformation into GVL catalysed by ZnAl mixed oxide, at 200ºC, using a FA/LA ratio 4/1. Symbols correspond to experimental points, whereas the broken lines correspond to the kinetic model proposed. Symbols: (●) LA; (▲) FA; (▲) AL; (◆) GVL.

The kinetic fit of the individual formic acid decomposition catalysed by ZnAl gives a kinetic rate of $k_1 = 8.2 \cdot 10^{-4} s^{-1}$, being the fitted data plotted in Fig. 2 in grey broken lines. This value is slightly higher than the one obtained in reaction conditions (red lines) and significantly higher than the rate obtained in the reaction of angelica lactone (green lines in Fig. 2, $k_1 = 4.5 \cdot 10^{-4}\ s^{-1}$). These results are explained considering the competitive adsorption of the formic acid and the other organic compounds involved in the reaction, being more relevant when angelica lactone is fed because of the stronger adsorption of this compound. The reaction of the angelica lactone intermediate was also fitted to the proposed model, obtaining a perfect fit with lower kinetic rates for all the steps involved in the main reaction ($k_2 = 3.7 \cdot 10^{-4}\ s^{-1}$, $k_3 = 1.24 \cdot 10^{-4}\ s^{-1}$, $k_4 = 3.2 \cdot 10^{-4}\ s^{-1}$, $k_5 = 3 \cdot 10^{5}\ s^{-1}$). This adjustment is shown as broken lines in Fig. 2, the black ones being the theoretical fit considering the values of kinetic rates for the main reaction. The discrepancy during the first 2 h suggests that the angelica lactone adsorption required to produce the reaction is stabilized by the presence of acidity in the reaction medium, needing a minimum of levulinic acid to promote the process.

3.3. Effect of reaction parameters.

The effect of temperature, as well as the initial FA/LA ratio in the catalytic activity of ZnAl mixed oxide, were simultaneously studied to analyse possible synergetic effects of these two variables, trying to identify the optimum conditions, i.e., maximum GVL with the minimum energetic and material costs. Main results after 6 h of reaction are summarized in **Figure 4**, where the effect of the five different ratios tested (from 1/1 to 5/1) and the three temperatures (80, 140 and 200ºC) is shown. The values of each

experiment are included in the supplementary information (**Table S1**). The carbon balance closure is not included in this analysis since all data are higher than 93 %, except for the reactions at 80ºC, with values from 76 to 92 %, discarding in the other cases a high relevance of side-reactions or adsorption process. In general terms, LA conversion increases as the temperature does, despite the FA/LA ratio used. In the same way, this conversion also increases with the ratio, despite the temperature. The second effect is more marked than the first one, in such a way that conversions higher than 80 % are reached with the ratio 5/1 at any temperature tested, whereas this value is only obtained at 200ºC when working at 4/1 ratio. On the contrary, even at the highest temperature, the LA conversion is limited to values lower than 60 % when using the equimolar ratio. The evolution with the temperature follows the anticipated trend of any kinetic reaction, whereas the strong influence of FA/LA reaffirms the previous hypothesis of equilibrium in the levulinic acid dehydration. According to this, a high amount of H_2 is required to displace the LA-AL equilibrium to the LA conversion by consuming the AL to produce GVL. This H_2 is obtained by the decomposition of FA, being this reaction strongly favoured by the excess of this acid.

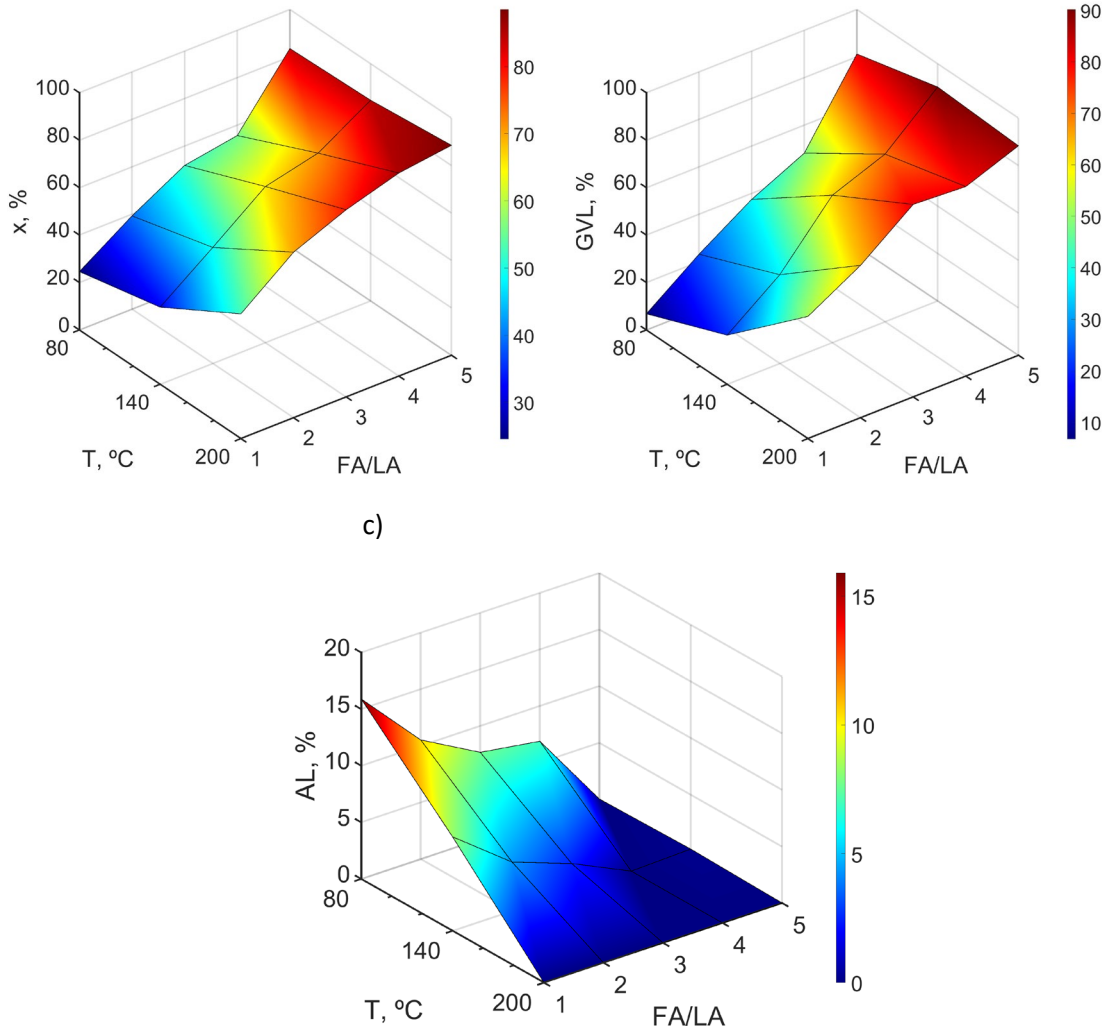

Figure 4: Analysis of (a) LA conversion; (b) GVL and (c) AL yields as function of the temperature and the initial FA/LA ratio

As it was previously observed, in formic acid excess conditions, the decomposition of FA with the ZnAl catalyst is strongly favoured, in such a way that there is a high correspondence between the LA conversion and the GVL yield and the AL intermediate is only observed in relevant amount (higher than 10 %) when working at the softest conditions, combining equimolar FA/AL ratio and temperatures below 140ºC. At these conditions, it is expected that the dehydration rate to be higher than the

hydrogenation one since total decomposition of FA is not reached (conversions of 69 % and 43 % at 140ºC and 80ºC, respectively). The kinetic of the hydrogenation is then identified as the limiting step, at these conditions. This result is congruent with the catalyst used since the absence of any metal nanoparticle could hinder the hydrogenation activity, prevailing the steps catalysed by acid sites.

Considering the balance between yields and costs, the range of optimum conditions includes ratios 4/1 (less excess of formic acid but high temperatures required) and 5/1 (high excess of formic acid but low dependence on the temperature). With slight differences as a function of these conditions, conversions higher than 83 % can be reached, with a minimum GVL yield of 80 %, and less than 5 % of AL detected as the only intermediate. These results correspond to carbon balance closures higher than 94 %, in all the cases. Decreasing the ratio to 3/1 implies working at 200^{o}C, observing a minimum decrease of 10 % in the LA conversion.

The role of temperature working at 5/1 is not significant, whereas preliminary results indicate a high relevance of this parameter when working in less FA excess (4/1). Thus, a deeper analysis of the temperature effect at 4/1 ratio was carried out, including studies at 100, 160 and 180^{o}C. The comparison of results after 6 h of reaction is included in **Figure 5**.

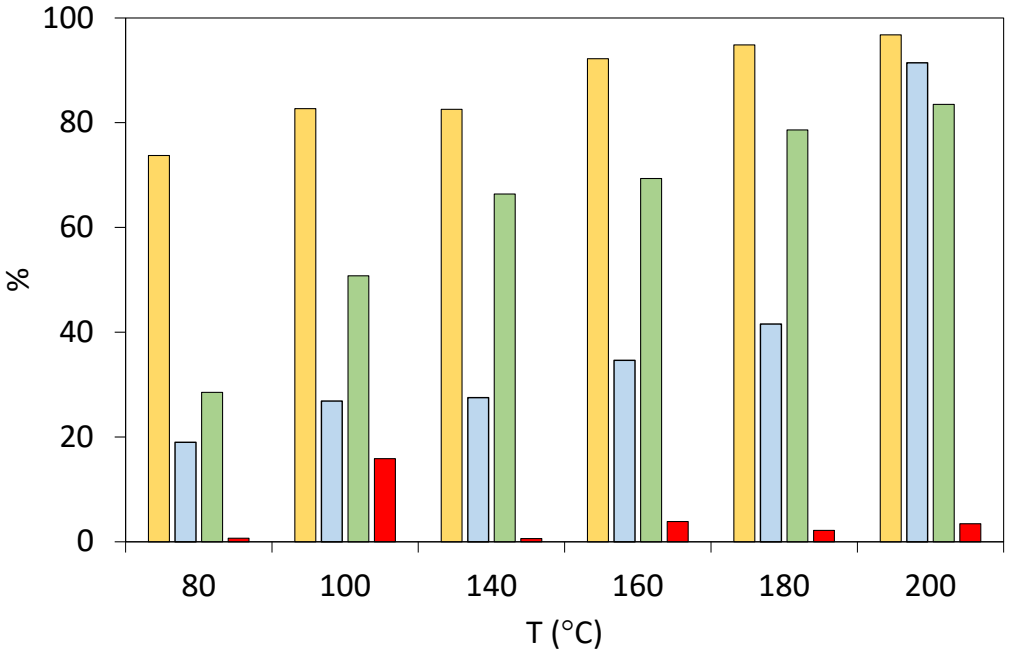

Figure 5: Comparison of levulinic acid conversion (yellow), formic acid conversion (blue), GVL yield (green), and angelica lactone yield (red)

Despite the high FA conversion obtained even at 80ºC (considering the high formic acid excess, 20 % of conversion could be enough to guarantee 80 % of GVL yield), a clear influence of temperature in this parameter is observed in the range 80-160ºC, with a relative increase in the LA conversion of 30 %, from 73 to 92 %. A more marked evolution is observed for the formic acid conversion, from 19 to 91 % in the considered range, the increase being strongly focused on the highest temperatures. Continuous evolution is observed for the GVL production, increasing from 28 to 83.4 %, at 80 and 200ºC, respectively. The maximum AL is observed at 100ºC, 15.8 %, in good agreement with a fast increase in the dehydration rate in this range. At higher temperatures, the increase in the hydrogenation rate is also evident, with a continuous decrease in the AL production, since almost all the intermediate is hydrogenated to GVL. All the carbon balance closures where higher than 97 %, except at 80ºC (76 %), fact that justifies the

low GVL yield observed at these conditions, concluding that the disappearance of levulinic acid involves not only reaction but also its adsorption on the catalytic surface.

Considering the previous literature of levulinic acid hydrogenation using formic acid as the hydrogen source, values obtained at 200ºC in this work can be only compared with those previously proposed with some noble metal catalysts such as Ru, Au supported on silica or zirconia (more expensive catalysts), with GVL yields higher than 95 % after 12 h at 150ºC [24], whereas these yields require higher temperatures if bifunctional materials, combining noble and transition metals, are used (Au-Ni, 220-285ºC) [24].

Experimental results were fitted according to the kinetic model previously proposed, obtaining the kinetic rates summarized in **Table 2**, whereas the correspondence between experimental and fitted values is plotted in **Figure 6**.

Table 2: Kinetic rates as function of the reaction temperature used in the levulinic acid hydrogenation catalysed by ZnAl mixed oxide as catalyst

Temperature (ºC)	k_1 ($L \cdot mol^{-1} \cdot s^{-1}$)	k_2 (s^{-1})	k_3 (s^{-1})	k_4 ($L \cdot mol^{-1} \cdot s^{-1}$)	k_5 (s^{-1})
80	$1.6 \cdot 10^{-6}$	$7.6 \cdot 10^{-5}$	$2.5 \cdot 10^{-6}$	$3.5 \cdot 10^{-4}$	$6.7 \cdot 10^{-8}$
100	$1.8 \cdot 10^{-5}$	$8.9 \cdot 10^{-5}$	$3.9 \cdot 10^{-6}$	$1.5 \cdot 10^{-3}$	$3.05 \cdot 10^{-6}$
140	$2.9 \cdot 10^{-5}$	$1.3 \cdot 10^{-4}$	$8.7 \cdot 10^{-5}$	$1.4 \cdot 10^{-2}$	$3.7 \cdot 10^{-5}$
160	$3.7 \cdot 10^{-5}$	$3.1 \cdot 10^{-4}$	$4.7 \cdot 10^{-4}$	$3.0 \cdot 10^{-2}$	$2.3 \cdot 10^{-4}$
180	$4.2 \cdot 10^{-4}$	$3.9 \cdot 10^{-4}$	$6.9 \cdot 10^{-4}$	$3.0 \cdot 10^{-2}$	$2.4 \cdot 10^{-4}$
200	$7.9 \cdot 10^{-4}$	$7.3 \cdot 10^{-4}$	$7.4 \cdot 10^{-4}$	$4.0 \cdot 10^{-2}$	$4.0 \cdot 10^{-4}$
Preexp. factor	$4.9 \cdot 10^{3}$	0.36	$3.9 \cdot 10^{5}$	$6.1 \cdot 10^{4}$	$3.5 \cdot 10^{7}$
Ea ($kJ \cdot mol^{-1}$)	63	25	76	54	96
r^2	0.88	0.90	0.95	0.96	0.94

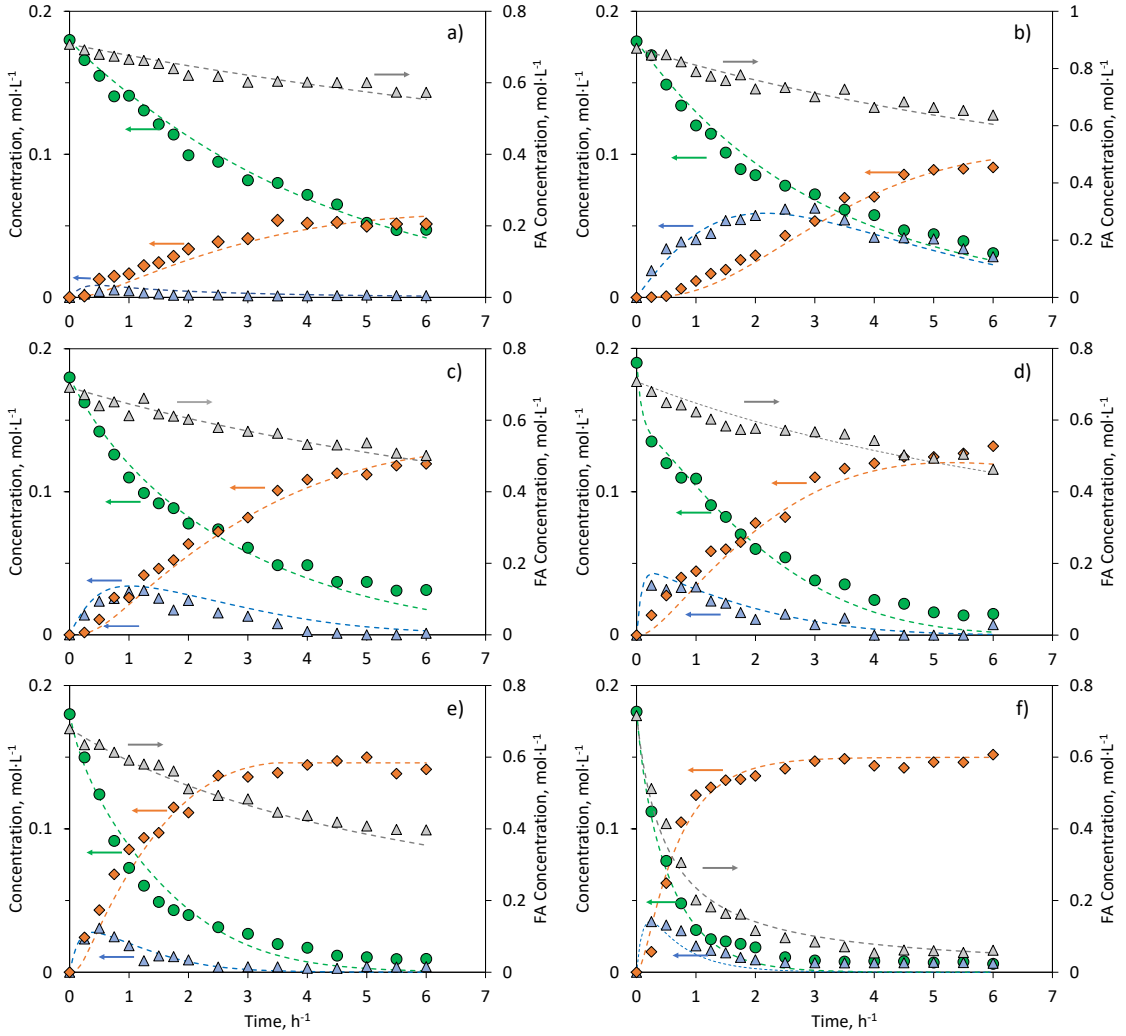

Figure 6. Temporal evolution of compounds involved in the LA transformation into GVL catalysed by ZnAl mixed oxide at (a) 80ºC; (b) 100ºC; (c) 140ºC; (d) 160ºC; (e) 180ºC; (f) 200ºC. Symbols correspond to experimental points, whereas the broken lines correspond to the kinetic model proposed. Symbols: (●) LA; (▲) FA; (▲) AL; (◆) GVL.

These values have a good fitting to an Arrhenius model, as shown in **Figure 7**.

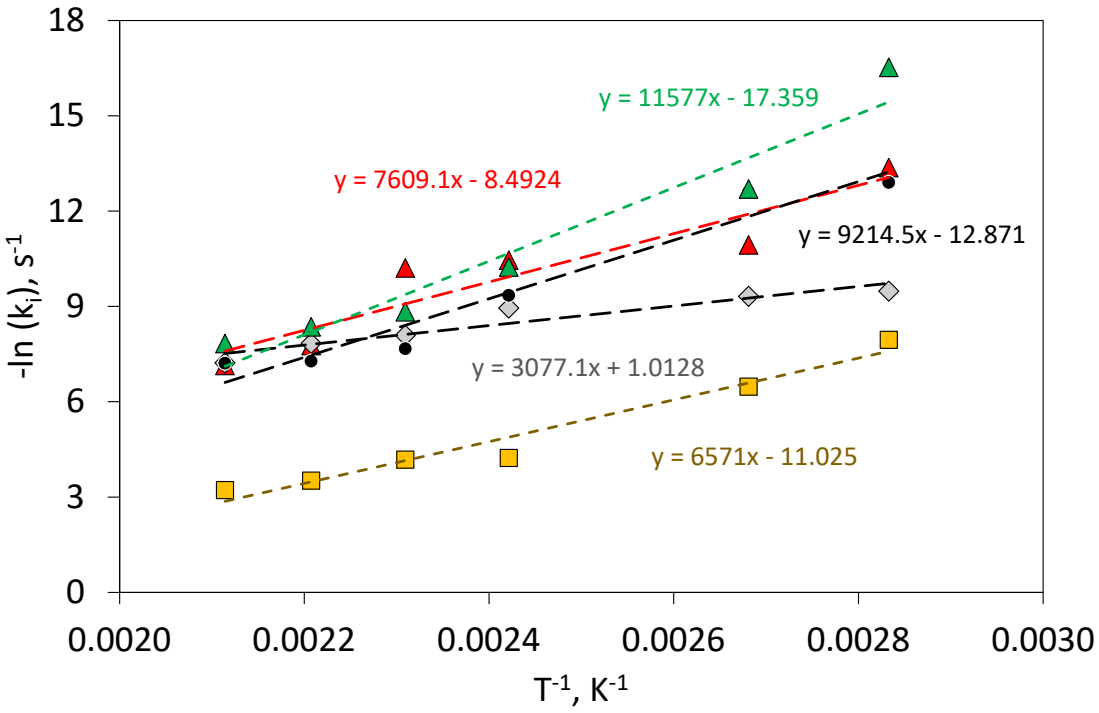

Figure 7: Arrhenius adjustment of kinetic rates obtained for the levulinic acid conversion catalysed by ZnAl mixed oxide. Data correspond to: (▲) k_1; (◆) k_2; (●) k_3; (■) k_4; and (▲) k_5.

As expected, considering the experimental data, the activation energy of the formic acid decomposition presents a low value (63 kJ/mol), in the same order of magnitude that values previously proposed for ZnO [29]. The worst correlation coefficient obtained for k_1 could be conditioned by a slight inaccuracy determining the hydrogen by a mass-balance since, despite the perfectly well-defined peaks obtained for formic acid, this compound has a high vapor pressure and a small fraction of this could be in the gas-phase. The prevalence of dehydration over hydrogenation steps is also explained by the lower activation energy of k_2, in comparison to the value of k_4. The low relevance of angelica lactone adsorption and subsequent oligomerization is

congruent with the high ratio k_4/k_5, in such a way that the hydrogenation prevails over this side-reaction.

These values also indicate that working at 200^{o}C does not imply a high relevance in the rates of main steps, whereas the reversible step, as well as the side reactions, increases at a higher extent. Considering these facts, the highest temperature is discarded. According to this, working at lower temperatures the differences between 4/1 and 5/1 increase in relevance and the best conditions correspond to the ratio 5/1, in this case working at 140^{o}C. In the basis of this premise, the optimum values are 84.5 % of conversion, with 90 % of GVL selectivity and less than 0.2 % of angelica lactone. To our best knowledge, these results are among the most promising ones for this reaction, with an optimum combination of cheap and high-available material (ZnAl mixed oxide) and mild reaction conditions.

3.4. Catalyst reusability

With the expectative of a future scale-up, catalyst recyclability is essential for ensuring the viability of the process. Different cycles of reaction were carried out, using for each run the catalyst previously separated from the previous cycle by filtration of the reaction medium, without any regeneration. The amounts of FA and LA were adjusted to keep constant the initial percentages (FA/LA = 5). Reactions were performed at 140^{o}C and main results are summarized in **Figure 8**. Results corresponding to angelica lactone are not included since values are always lower than 0.2 %. There is a continuous but slight decrease in the LA conversion during the first four cycles, the fourth one is 15 % lower than the first cycle. In the two first reuses, a good carbon

balance closure discards a high relevance of side reactions. However, the evolution during the third and fourth cycle, with a decrease in this magnitude, suggests that these side reactions were taking place, but they are only relevant once the deposits have blocked enough amount of active sites to conditions the global activity. According to these results, levulinic acid is being directly or indirectly deposited on the catalytic surface.

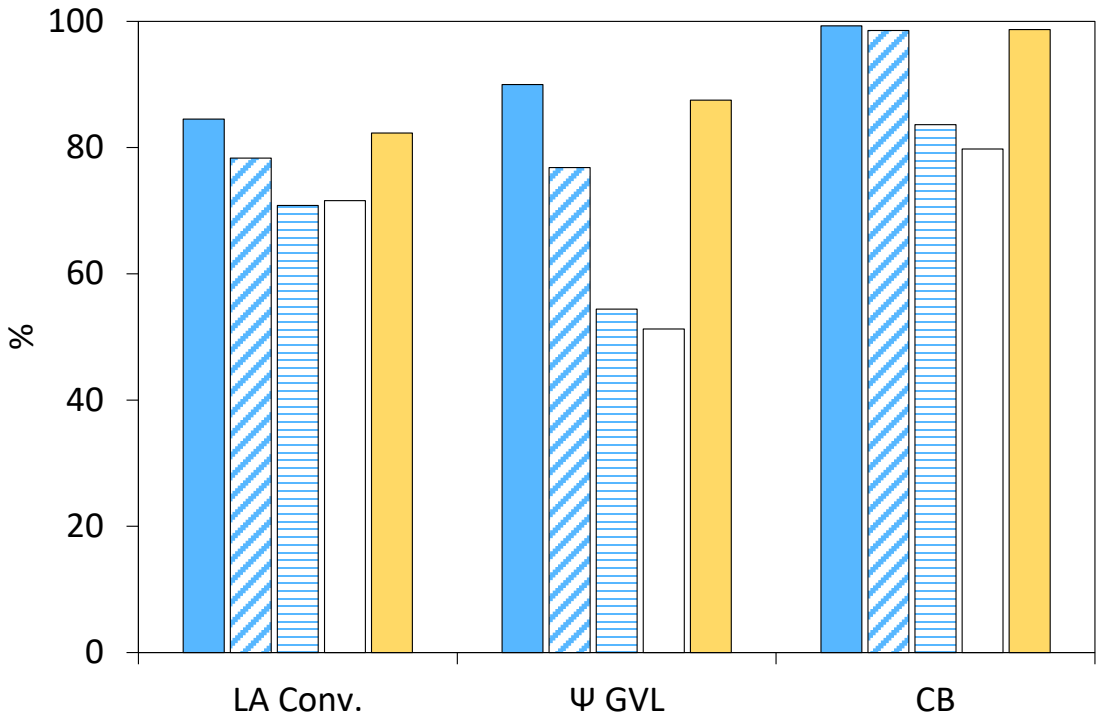

Figure 8: Catalytic reusability of ZnAl with a FA/LA ratio 5/1 at 140^{o}C. Values corresponding to first (filled bars), second (diagonal bars), third (horizontal bars), and fourth (white bars) cycles. Orange bars correspond to data after the catalytic regeneration.

To analyse the deactivation causes, TPO analyses of catalyst after the first and fourth cycle were done. Results after the fourth cycle are shown in **Figure 9**, whereas there

was not any significant signal in the analysis after the first cycle. In this figure, the spectra were deconvoluted into three relevant signals, with oxidation temperatures of 325, 430 and 510ºC. These values are like the previous ones obtained for NiAl mixed oxide, suggesting that the nature of these solids is quite similar, related to AL oligomerization. Thus, the slight differences could be justified by the different interactions between these oligomers and the mixed oxide structures. The low adsorption observed in the first cycle seems to be enough to promote exponential adsorption in the consecutive cycles, resulting in a relevant deactivation in future cycles. Thus, the minimization of this formation will lead not only to higher yields to the desired product but also to more stable catalyst performance.

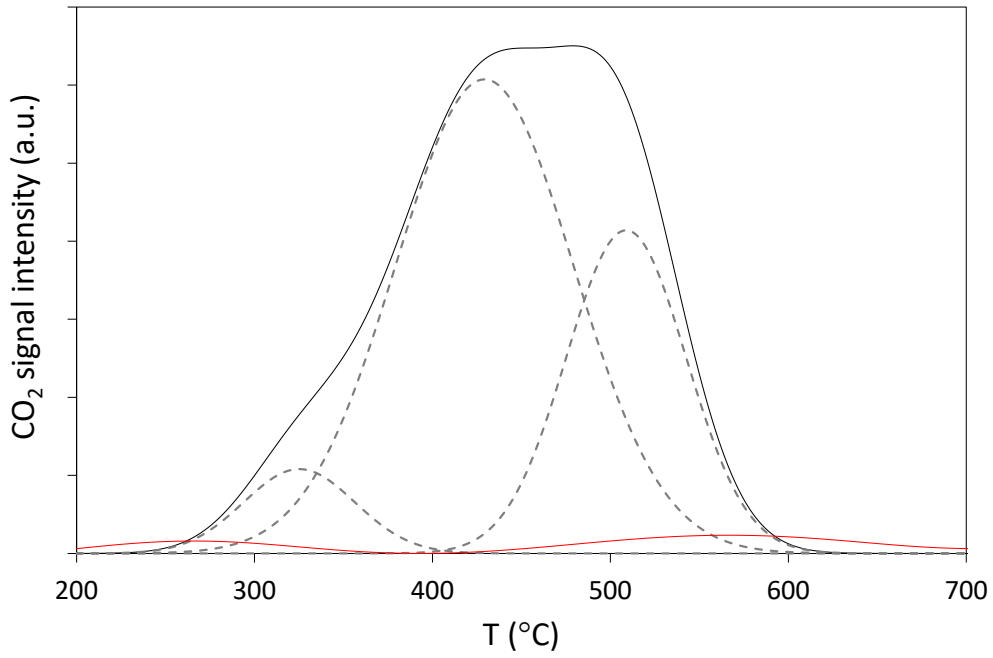

Figure 9: TPO spectra of m/z 44 after the first (red) and fourth (black) cycles of levulinic acid hydrogenation catalysed by ZnAl using formic acid as H_2 source (FA/LA = 5/1, 140ºC). The grey broken lines correspond to the deconvoluted peaks of the three main carbonaceous contributions

The acidic hydrothermal conditions could lead to the formation of coke, obtaining a solid deposit whose exact structure has not been accurately worked out [45]. However, the soft oxidation temperatures of these deposits suggest that this mixed oxide can be effectively regenerated by calcination. Thus, the used catalyst recovered after the fourth cycle was calcined at 600^{o}C (temperature needed, according to the TPO, for removing all the organic deposits) and the resulting catalyst was tested providing similar results than those obtained with the same amount of fresh catalyst. These results are included also in Figure 9.

CONCLUSIONS

ZnAl mixed oxide exhibited a high performance on the catalytic hydrogenation of levulinic acid using formic acid as the hydrogen source. Under the optimum conditions (140ºC, formic/levulinic acid ratio 5/1), 90 % of GVL yield is reached, with more than 87 % of levulinic conversion in less than 6 h and a carbon balance higher than 95 %, values significantly better than those proposed in the literature for these conditions.

The high dehydrogenation capacity of ZnO phases is identified as the key parameter of the process. In addition, a good hydrogenation capacity is required to prevent a high production of angelica lactone, since the levulinic acid dehydration is the fastest step. This intermediate must be reduced since its oligomerization, catalysed by strong basic sites, is the main deactivation cause.

Experimental results were fitted to a kinetic model considering a bimolecular reaction for the formic acid decomposition, and first-order equations for the subsequent steps.

The levulinic acid dehydration is believed as a reversible step, in good agreement with experimental results. Activation energy obtained for the hydrogenation formation catalysed by ZnAl is in the order of those obtained with noble metals.

ACKNOWLEDGMENTS

This study has been financial supported by the Spanish Ministry of Economy and Competitiveness (CTQ2017-89443-C3-2-R). Meriem N.E.H. Belguendouz gratefully acknowledges to the High Teaching and Scientific Research ministry, Algeria, its PhD fellowship (PNE).

References

[1] D. Martin Alonso, S.G. Wettstein, J.A. Dumesic, Gamma-valerolactone, a sustainable platform molecule derived from lignocellulose biomass. Green Chem. 15 (2013) 584-595. https://doi.org/10.1039/C3GC37065H

[2] S. Ghysels, A.E.E. León, M. Pala, K.A. Schoder, J.Van Acker, F. Ronsse, Fast pyrolysis of mannan-rich ivory nut (Phytelephas aequatorialis) to valuable biorefinery products. Chem. Eng. J. 373 (2019) 446-457. https://doi.org/10.1016.j.cej.2019.05.042

[3] L. Zhang, G. Xi, Z. Chen, D. Jiang, H. Yu, X. Wang, Highly selective conversion of glucose into furfural over modified zeolites. Chem. Eng. J. 307 (2017) 868-876. https://doi.org/10.1016/j.cej.2016.09.001

[4] C. Liu, M. Wei, J. Wang, J.M. Xu, J.C. Jiang, K. Wang, Facile directional conversion of cellulose and bamboo meal wastes over low-cost sulfate and

polar aprotic solvent. ACS Sust. Chem. Eng. 8 (2020) 5776-5786. https://doi.org/10.1021/acssuschemeng.0c01280.

[5] O. Nakayama, Manufacture of delta-valerolactone derivative used as intermediate component for pharmaceutical, agrochemical, cosmetics and food additive, involves reacting epoxy alcohol compound and carbon monoxide in presence of cobalt compound. JP2008050318-A

[6] S. Tanaka, K. Fukuda, T. Asada. New valerolactone compounds are perfumes for use in e.g. perfumes, cosmetics, foods and pharmaceuticals. WO2004029033-A1

[7] B.M. Stadler, A. Brandt, A. Kux, H. Beck, J.G. de Vries, Properties of novel polyesters made from renewable 1,4-pentanediol. ChemSusChem 13 (2020) 556-563. https://doi.org/10.1002/cssc.201902988

[8] Y. Yang, X.R. Wei, F.X. Zeng, L. Deng, Efficient and sustainable transformation of gamma-valerolactone into nylon monomers. Green Chem. 18 (2016) 691-694. https://doi.org/10.1039/C5GC01922B

[9] D. Sun, T. Saito, Y. Yamada, X. Chen, S. Sato, Hydrogenation of γ-valerolactone to 1,4-pentanediol in a continuous flow reactor. Appl. Catal. A 542 (2017) 289-295. https://doi.org/10.1016/j.apcata.2017.05.034

[10] Y.X. Jing, Y. Guo, Q.N. Xia, X.H. Liu, Y.Q. Wang, Catalytic production of value-chemicals and liquid fuels from lignocellulosic biomass. Chem 5 (2019) 2520-2546. https://doi.org/10.1016/j.chempr.2019.05.022

[11] I.T. Horváth, H. Mehdi, V. Fábos, L. Boda, L.T. Mika, γ-Valerolactone – a sustainable liquid for energy and carbon-based chemicals. Green. Chem. 10 (2008) 238-242. https://doi.org/10.1039/B712863K

[12] D. Garcés, L. Faba, E. Díaz, S. Ordóñez, Aqueous phase transformation of glucosa into hydroxymethylfurfural and levulinic acid by combining

homogeneous and heterogeneous catalysis. ChemSusChem 12 (2019) 924-934. https://doi.org/10.1002/cssc.201802315.

[13] M. Ojeda, E. Iglesia, Angew. Formic acid dehydrogenation on Au-based catalysts at near-ambient temperatures. Chem. Int. Ed. 48 (2009) 4800-4803. https://doi.org/10.1003/anie.200805723

[14] S. Dutta, I.K.M. Yu, D.C.W. Tsang, Y.H Ng, Y.S. Ok, J. Sherwood, J.H. Clark, Green synthesis of gamma-valerolactone (GVL) through hydrogenation of biomass-derived levulinic acid using non-noble metal catalysts: a critical review. Chem. Eng. J. 372 (2019) 992-1006. https://doi.org/10.1016/j.cej.2019.04.199

[15] W.R.H. Wright, R. Palkovits, Development of heterogeneous catalysts for the conversion of levulinic acid to γ-valerolactone. ChemSusChem 5 (2012) 1657-1667. https://doi.org/10.1002/cssc.201200111.

[16] O.A. Abdelrahman, A. Heyden, J.Q. Bond, Analysis of kinetics and reaction pathways in the aqueous-phase hydrogenation of levulinic acid to form γ-valerolactone over Ru/C. ACS Catal. 4 (2014) 1171-1181. https://doi.org/10.1021/cs401177p.

[17] S. Xu, D. Yu, T. Ye, P. Tian, Catalytic transfer hydrogenation of levulinic acid to γ-valerolactone over a bifunctional tin catalyst. RSC Adv. 2 (2017) 1026-1031. https://doi.org/10.1039/C6RA25594A.

[18] R. Xu, K. Liu, H. Du, H. Liu, X. Cao, X. Zhao, G. Qu, X. Li, B. Li, C. Si, Falling leaves return to their roots: a review on the preparation of γ-valerolactone from lignocellulose. ChemSusChem (2020) *In press*. https://doi.org/10.1002/cssc.202002008.

[19] R. Sivec, M. Grilc, M.Hus, B. Likozar, A review of multi-scale modelling of (hemi)cellulose hydrolysis and cascade hydrotreatment of 5-HMF, furfural and levulinic acid. Ind. Eng. Chem. Res. 58 (2019) 16018-16032. https://doi.org/10.1021/acs.iecr.9b00898.

[20] M. Grilc, B. Likozar, Levulinic acid hydrodeoxygenation, decarboxylation and oligomerization over NiMo/Al_2O_3 catalyst to bio-based value-added chemicals: modelling of mass transfer, thermodynamics and micro-kinetics. Chem. Eng. J. 330 (2017) 383-397. https://doi.org/10.1016/j.cej.2017.07.145.

[21] M. Grlick, B. Likozar, J. Levec, Hydrotreatment of solvolytically liquified lignocellulosic biomass over NiMo/Al2O3 catalyst: reaction mechanism, hydrodeoxygenation kinetics and mass transfer model based on FTIR. Biomass Bionerg. 63 (2014) 300-312. https://doi.org/10.1016/j.biombioe.2014.02.014

[22] S. Lomate, A. Sultana, T. Fujitani, Vapor phase catalytic transfer hydrogenation (CTH) of levulinic acid to γ-valerolactone over copper supported catalysts using formic acid as hydrogen source. Catal. Lett. 148 (2018) 348-358. https://doi.org/10.1007/s10562-017-2241-z.

[23] M.J. Hidajat, A. Riaz, J. Kim, A two-step approach for producing oxygen-free aromatics from lignin using formic acid as a hydrogen source. Chem. Eng. J. 348 (2018) 799-810. https://doi.10.1016/j.cej.2018.05.0136.

[24] Z. Yu, X. Lu, J. Xiong, X. Li, H. Bai, N. Ji, Heterogeneous catalytic hydrogenation of levulinic acid to γ-valerolactone with formic acid as internal hydrogen source: key issues and their effects. ChemSusChem 13 (2020) 2916-2930. https://doi.org/10.1002/cssc.202000175.

[25] M. Chia, J.A. Dumesic, Liquid-phase catalytic transfer hydrogenation and cyclization of levulinic acid and its esters to γ-valerolactone over metal oxide catalysts. Chem Commun. 47 (2011) 12233-12235. https://doi.org/10.1039/c1cc14748j.

[26] Y. Kuwahara, W. Kaburagi, Y. Osada, T. Fujitani, H. Yamashita, Catalytic transfer hydrogenation of biomass-derived levulinic acid and its esters to gamma-valerolactone over ZrO_2 catalyst supported on SBA-15 silica. Catal. Today 281 (2017) 418-428. https://doi.org/10.1016/j.cattod.2016.05.016.

[27] C. Xu, E. Paone, D. Rodríguez-Padrón, R. Luque, F. Mauriello, Recent catalytic routes for the preparation and the upgrading of biomass derived furfural and 5-hydroxymethylfurfural. Chem. Soc. Rev. 49 (2020) 4273-4306. https://doi.org/10.1039/d0cs00041h.

[28] O. Sneka-Platek, K. Kazmierczak, M. Jedrzejczyk, P. Sautet, N. Keller, C. Michel, P. Sautet, N. Keller, C. Michel, A.M. Ruppet, Understanding the influence of the composition of the Ag-Pd catalysts on the selective formic acid decomposition and subsequent levulinic acid hydrogenation. Int. J. Hyd. Energ. 45 (2020) 17339-17353. https://doi.org/10.1016/j.ijhydene.2020.04.180.

[29] M. Yoshimoto, S. Takagi, Y. Umemura, M. Hada, H. Nakatsuji, Theoretical study on the decomposition of HCOOH on a ZnO(1010) surface. J. Catal. 173 (1998) 53-63. https://doi.org/10.1006/jcat.1997.1889.

[30] H.C. Genuino, H. H. van de Bovenkamp, E. Wilbers, J.G.M. Winkelman, A. Goryachev, J.P. Hofmann, E.J.M. Hensen, B.M. Weckhuysen, P.C.A.Bruijnincs, H.J. Heeres, Catalytic hydrogenation of renewable levulinic acid to γ-valerolactone: insights into the influence of feed impurities on catalyst performance in batch and flow reactors. ACS Sust. Chem. Eng. 8 (2020) 5903-5919. https://doi.org/10.1021/acssuschemeng.9b07678.

[31] X.-L Du, L. He, S. Zhao, Y.-M. Liu, Y. Cao, H.-Y. He, K.-N. Fan. Hydrogen-independent reductive transformation of carbohydrate biomass into γ-valerolactone and pyrrolidone derivatives with supported gold catalysts. Angew. Chem. Int. Ed. 40 (2011) 7815-7819. https://doi.org/10.1002/anie.201100102.

[32] Y. Gao, H. Zhang, A. Han, J. Wang, H.R. Tan, E.S. Tok, S. Jaenicke, G.K. Chuah, Ru/ZrO_2 catalysts for transfer hydrogenation of levulinic acid with formic acid/formate mixtures: importance of support stability. ChemistrySelect 3 (2018) 1343-1351. https://doi.org/10.1002/slct.201702152.

[33] A. M. Ruppert, M. Jedrzejczyk, N. Potrzebowska, K. Kazmierczak, M. Brzezinska, O. Sneka-Platek, P. Sautet, N. Keller, C. Michel, J. Grams, Supported gold-nickel nano-alloy as a highly efficient catalyst in levulinic acid hydrogenation with formic acid as an internal hydrogen source. Catal. Sci. Technol. 8 (2018) 4318-4331. https://doi.org/10.1039/c8cy00462e.

[34] R. Yoshida, D. Sun, Y. Yamada, S. Sato, G.J. Hutchings, Vapor-phase hydrogenation of levulinic acid to γ-valerolactone over Cu-Ni bimetallic catalysts. Catal. Commun. 97 (2017) 79-82. https://doi.org/10.1016/j.catcom.2017.04.018.

[35] O. Vozniuk, T. Tabanelli, N. Tanchoux, J.M.M. Millet, S. Albonetti, F. Di Renzo, F. Cavani. Mixed-oxide catalysts with spinel structure for the valorization of biomass: the chemical-loop reforming of bioethanol. Catalysts 8 (2018) 332. https://doi.org/10.3390/catal8080332.

[36] L. Faba, E. Díaz, S. Ordóñez, Base-catalyzed reactions in biomass conversion: reaction mechanisms and catalyst deactivation. In Reaction Pathways and mechanisms in thermocatalytic biomass conversion I: cellulose structure, depolymerization and conversion by heterogeneous catalysts. Ed. Springer, 2016, 87-122. https://doi.org/10.1007/978-287-68-1_5.

[37] S.K. Hussain, V.K. Velisoju, N.P. Rajan, B.P. Kumar, K.V.R. Chary, Synthesis of γ-valerolactone from levulinic acid and formic acid over Mg-Al hydrotalcite like compound. Chem. Select 3 (2018) 6186-6194. https://doi.org/10.1002/slct.201800536.

[38] K. Li, H.J. Sun, W.J. Yang, Y.J. Wang, S. Q. Xie, X.Y. Li, O. Fuhr, D. Fenske, Efficient dehydration of primary amides to nitriles catalyzed by phosphorus-chalcogen chelated iron hydrides. Appl. Organomet.. Chem. 34 (2020) e5337. https://doi.org/10.1002/aoc.5337.

[39] B. Sabour, M.H. Peyrovi, T.Hamoule, M. Rashidzadeh, Catalytic dehydration of methanol to dimethyl ether (DME) over Al-HMS catalysts. J. Ind. Eng. Chem. 20 (2014) 222-227. https://doi.org/10.1016/j.jiec.2013.03.044.

[40] J.A. Nasir, M. Hafeez, M. Arshad, N.Z. Ali, I.F. Teixeira, I. McPherson, Z. Rehman, M.A. Khan, Photocatalytic dehydrogenation of formic acid on CdS nanorods though Ni and Co redox mediation under mild conditions. ChemSusChem 11 (2018) 2587-2592. https://doi.org/10.1002/cssc.201800583.

[41] G. Wang, Z.X. Li, C.S. Li, S.J. Zhang, Preparation of methyl acrylate from methyl acetate and methanol with mild catalysis of cobalt complex. Chem. Eng. J. 359 (2019) 863-873. https://doi.org/10.1016/j.cej.2018.11.106.

[42] L. Faba, E. Díaz, S. Ordóñez, Gas phase acetone self-condensation over unsupported and supported Mg-Zr mixed-oxides catalysts. Appl. Catal. B 113-142 (2013) 387-395. https://doi.org/10.1016/j.apcatb.2013.05.043.

[43] L. Faba, E. Díaz, S. Ordóñez, Hydrodeoxygenation of acetone-furfural condensation adducts over alumina-supported noble metal catalysts. Appl. Catal. B 113-160 (2014) 436-444. https://doi.org/10.1016/j.apcatb.2014.05.053.

[44] H.S. Fogler, Elements of Chemical Reaction Engineering. Pearson Education (2016).

[45] A. Dell'Acqua, B. M. Stadler, S. Kirchhecker, S. Tin, J.G. de Vries, Scalable synthesis and polymerization of a β-angelica lactone derived monomer. Green Chem. (2020). https://doi.org/10.1039/d0gc00338g.

[46] M. Novozhilova, D. Anischenko, I. Chepurnaya, E. Dmitrieva, V. Malev, A. Timonov, M. Karushev. Metal-centered redox activity in a polymeric cobalt (II) complex of a sterically hindered salen type ligand. Electrochem. Act. 353 (2020) 136496. https://doi.org/10.1016/j.electacta.2020.136496.

[47] G. García, R. Sanchís, F.J. Llopis, I. Vázquez, M.P. Pico, M.L. López, I. Álvarez-Serrano, B. Solsona, Ni supported on natural clays as a catalyst for the transformation of levulinic acid into gamma-valerolactone without the addition of molecular hydrogen. Energies 13 (2020) 3448-3465. https://doi.org/10.3390/en13133448.

[48] P. Zhang, C.H. Liu, L. Chen, J.M. Chen, Y. Guan, P. Wu, Factors influencing the activity of SiO2 supported bimetal Pd-Ni catalyst for hydrogenation of α-angelica lactone: oxidation state, particle size, and solvents. J. Catal. 351 (2017) 10-18. https://doi.org/10.1016/j.jcatal.2017.04.017.

[49] B. Wei, J. Chen, M. Mavrikakis, Formic acid: a hydrogen-gonding cocatalyst for formate decomposition. ACS Catal. 10 (2020) 10812-10825. https://doi.org/10.1021/acscatal.0c02902.

[50] D. Sun, Y. Takahashi, Y. Yamada, S. Sato, Efficient formation of angelica lactones in a vapor-phase conversion of levulinic acid. Appl. Catal. A 526 (2016) 62-69. https://doi.org/10.1016/j.apcata.2016.07.025.

[51] Y. Shi, X. Li, X. Rong, B. Gu, H. Wei, C. Sun, Influence of support on the catalytic properties of Pt-Sn-K/θ-Al2O3 for propane dehydrogenation. RSC Adv. 7 (2017) 19841-19848. https://doi.org/10.1039/c7ra02141k.

[52] B. Li, G.S. Hu, L.Y. Jin, X. Hong, J.Q. Lu, M.F. Luo, Characterizations of Ru/ZnO catalysts with different Ru contents for selective hydrogenation of crotonaldehyde. J. Ind. Eng. Chem. 19 (2013) 250-255. https://doi.org/10.1016/j.jiec.2012.08.008.